Anomalous velocity fluctuation in one-dimensional defect turbulence

Yusuke Uchiyama, Takanori Kadoya, and Hidetoshi Konno
Department of Risk Engineering, Faculty of Information and Systems, University of Tsukuba, Tsukuba, Ibaraki 305-8573, Japan
(Received 27 July 2014; published 19 February 2015)

In this paper various eccentric hole dynamics are presented in defect turbulence of the one-dimensional complex Ginzburg-Landau equation. Each hole shows coherent particlelike motion with nonconstant velocity. On the other hand, successive hole velocities without discriminating each hole exhibit anomalous intermittent motions being subject to multi-time-scale non-Gaussian statistics. An alternate non-Markov stochastic differential equation is proposed, by which all these observed statistical properties can be described successfully.

DOI: 10.1103/PhysRevE.91.022127 PACS number(s): 02.50.−r, 05.40.−a, 05.90.+m, 89.75.Kd

I. INTRODUCTION

Particle velocity fluctuations in equilibrium systems, such as ideal gases, are subject to the Maxwell-Boltzmann law [1]. This is one of the main consequences of equilibrium statistical mechanics. However, velocity fluctuations in nonequilibrium systems, where energy and/or momentum exchange, exhibit abundant anomalous behaviors being subject to non-Gaussian statistics with large deviations. Many-body interactions among collective inelastic gases, where momentum decreases after collision, display Lévy type velocity distributions [2]. In general, topological defects in phase-ordering systems have velocity distributions with fat tails [3]. Lagrangian particles in porous media show intermittent motions with long-time rests, for which the velocity distribution is also characterized by large deviations [4].

In order to understand the common nature of nonequilibrium systems, one aspires to deal with a minimal model describing spatiotemporal dynamics which can be observed everywhere. Mathematical models such as amplitude equations have been derived from original equations by the reductive perturbations methods or the method of multiple scales. The complex Ginzburg-Landau equations (CGLE) have been introduced to describe spatiotemporal dynamics in oscillatory media with weak nonlinearity associated with supercritical Hopf bifurcations [5–7]. When the CGLE is not enough to describe more complicated spatiotemporal dynamics, such as hexagonal pattern formations related to non-Boussinesq convection (e.g., Ref. [8]), coupled CGLEs and/or complex Swift-Hohenberg equation [5,7,9] and their modifications must be introduced. In particular, defect velocity fluctuations have been extensively investigated with the help of the two-dimensional (2D) CGLE. In inclined layer thermal fluid convection, non-Gaussian defect velocity distributions have been observed experimentally [10], and have been identified by the theoretical framework of nonextensive statistical mechanics [11]. On the other hand, a non-Gaussian velocity distribution have been derived from a one-dimensional (1D) transport equation [12]. We have introduced appropriate identification methods for local structures, which are localized nonlinear waves in 1D systems, such as the defect, the hole, and the modulated amplitude wave, and have investigated their statistical characteristics [13]. Using the method, we have tracked successfully each hole in the defect turbulence and have speculated that the hole velocity distribution can be described by a generalized Cauchy distribution [14].

While the anomalous velocity distributions at steady states have been investigated in many systems, their dynamical properties, such as autocorrelation function (ACF) and mean-square displacement (MSD), have yet to be described by a unified theoretical model. In other words, dynamical stochastic models of the abundant anomalous velocity fluctuations remain to be fully elucidated. In many previous works, these dynamical properties and probability distributions for random fluctuations have been studied separately.

The ACF for a stochastic process has been used to investigate the existence of long memory, which is characterized by a power-law decay. As such, stochastic models with long memory, generalized Langevin equations [15], continuous time random walks [16], time fractional Fokker-Planck equations [17], and nonstationary master equations [18] have been developed. As far as we know, the MSDs of these stochastic models show subdiffusive behaviors since long memory in many systems can be ascribed to frequently trapped particle motions in their transport processes [16,17,19].

Recently, many theoretical probability distributions have been proposed for describing "large deviations" in statistics, i.e., probability density functions (PDFs) with fat tails. As far as the mathematical fitting of empirical data to the PDF is concerned, one can fit experimental or simulated PDF with one of the probability distributions.

"On the theory of Tsallis statistics" [20], (i) there is an *ad hoc* parameter q; (ii) the physical origin of the corresponding nonlinear Fokker-Planck equation (NLFPE) is not clear. Actually, Grassberger pointed out the deficiency of Tsallis's theory [21], although the features of anomalous diffusion can be derived from the NLFPE.

To identify the physical origin of large deviations in statistics, Beck and Cohen have developed the superstatistics [22] where original state variables are decomposed of random variables in local thermal equilibrium and slowly fluctuating inverse temperatures. However, the ACF of the original state variables cannot be predicted since the superstatistics is not related explicitly to a specified Fokker-Planck equation or a Langevin equation.

We utilized a class of generalized Cauchy processes (GCPs) [23] to construct an alternate stochastic model in describing both the PDF and the ACF of hole velocity fluctuation in the defect turbulence of the 1D CGLE. The feature of anomalous diffusion in the GCP depends on the value of its parameters and dimensions [24].

In this study, we investigate the hole dynamics in the defect turbulence of the 1D CGLE, and present the unified stochastic model for the hole velocity fluctuation involved in the PDF, the ACF, and the MSD. Section II presents a brief explanation of our numerical simulation for the 1D CGLE and the identification method of holes in the defect turbulence. Section III presents a hole tracking procedure and some sample trajectories of the holes, which display particlelike motions. In Sec. IV, without discriminating each hole, successive hole velocities are investigated as a random time series, and their unified stochastic model is presented. Section V is devoted to conclusions and future perspectives.

II. NUMERICAL SIMULATION AND HOLE IDENTIFICATION

The CGLE is derived from a nonlinear partial differential equation having dissipation terms near a supercritical Hopf bifurcation [5–7]. A rescaled form of the dimensionless CGLE in terms of a complex order parameter A with two real parameters c_1 and c_2 is given by

$$\partial_t A = A + (1 + ic_1)\nabla^2 A - (1 + ic_2)|A|^2 A. \qquad (1)$$

Depending on the values of c_1 and c_2, the CGLE shows rich spatial or spatiotemporal patterns in any dimensions [25,26].

We implemented a numerical simulation of the 1D CGLE in the regime of defect turbulence. The initial condition is given by $A_0(x) = \xi_1 + \tanh(x)\exp[i(x + \xi_2)]$, where ξ_1 and ξ_2 are Gaussian random numbers with null means whose variances are 0.1 or 0.01, respectively. We confirmed that the change of the initial condition does not alter the spatiotemporal dynamics after transient dynamics. In order to trace the motions of holes more accurately, it is preferable to guarantee spectral accuracy for space with a finer grid. Therefore, we employed a split-step Fourier method with fourth-order accuracy for time in the system $\Omega = 80\pi$, subject to a periodic boundary condition [27]. Time and space resolutions were fixed to $\Delta t = 10^{-3}$ and $\Delta x = 2^{-12}\times\Omega$, respectively. The parameter values in Eq. (1) were chosen to produce the defect turbulence with $(c_1, c_2) = (1.5, -1.2)$. Note that this change of numerical scheme and system size does not affect the qualitative statistical law of the defect turbulence previously reported [13].

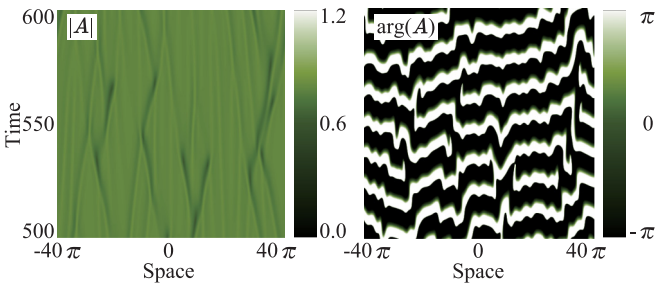

FIG. 1. (Color online) Spatiotemporal profiles of amplitude $|A|$ and phase arg (A) in the whole system. In the amplitude profile, black lines indicate trajectories of locally depressed amplitude. In the phase profile, slits correspond to phase discontinuities.

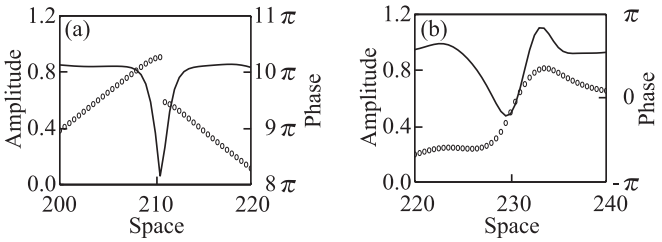

FIG. 2. Snapshots of (a) a defect and (b) a hole. Black lines and white circles are amplitude and phase, respectively. The defect has a phase singularity at its core, whereas the hole does not have the same feature.

Figure 1 shows the pseudocolor plots for spatiotemporal profiles of amplitude $|A|$ and phase arg(A). In the amplitude profile, black lines indicate trajectories of locally depressed amplitude. In the phase profile, slits correspond to phase discontinuities. These two characteristics are an expression of a well-known phase singularity of the 1D CGLE, i.e., the Bekki-Nozaki (BN) hole [28]. On the other hand, another hole without phase singularity has been presented as a specific form of traveling waves, defined as the homoclinic hole [29]. Thus these two distinct holes have to be discriminated clearly to understand the true nature of the defect turbulence.

In our previous work [13], we proposed appropriate identification methods of the two distinct holes, carried out discrimination between them, and tagged the BN hole and the homoclininc hole as a *defect* and a *hole*, respectively, in the defect turbulence. Based on the identification methods, stochastic dynamics of birth-death processes of both holes and modulated amplitude waves in defect turbulence have been unveiled to show Poisson processes with long memory, which is described successfully by a nonstationary master equation. However, a naive identification method of holes with only amplitude gives sub-Poisson statistics in hole number fluctuations [30], which is an illusion or an artifact.

A defect is identified as a local minimum of amplitude with a phase singularity in $x - t$ plane, and a hole is captured as one not having the same feature. Figure 2 shows snapshots of a defect and a hole, with solid lines denoting amplitude, and white circles denoting phase. It is recognized that the defect has phase discontinuity at its amplitude minimum, whereas the hole does not have the same feature. Reflecting the fact that the BN hole is structurally unstable, namely, it collapses under a perturbation [31], the lifetime of a defect is shorter than the time step of the numerical simulation Δt, and thus does not show any motion. Hence we can only track trajectories of the holes in the defect turbulence.

III. HOLE TRAJECTORIES

After identifying the holes, we tracked their trajectories during their lifetimes. The trajectories are restricted by the temporal and the spatial resolutions of the numerical simulation, which is to say that the holes can only move to the nearest-neighbor pixels at each time step. In order to reduce the influence of the spatiotemporal resolutions on the trajectories, we replaced the hole positions with their weighted average. The weighting function for a hole position x_i at time t_i affected

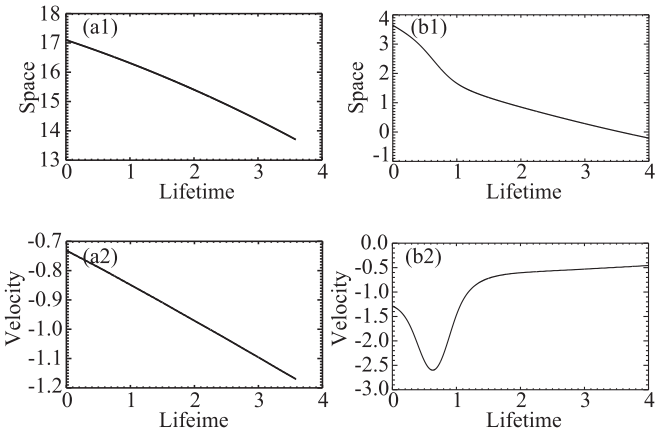

FIG. 3. Sample hole trajectories with their velocity diagrams. The hole trajectories in (a1) and (b1) were obtained by the smoothing with the weighting function. The hole velocities in (a2) and (b2) were evaluated by the local regression at each point in (a1) and (b2), respectively.

by other sets of position and time (x_j,t_j) is given by the Gaussian function as $w_{ij} = (2\pi\sigma_x\sigma_t)^{-1}\exp[-2^{-1}\{\sigma_x^{-2}(x_i - x_j)^2 + \sigma_t^{-2}(t_i - t_j)^2\}]$ with $\sigma_x^2 = 2\Delta x$ and $\sigma_t^2 = 2\Delta t$ [32]. From the smoothed trajectory with coordinates $\hat{x}_i = \sum_j w_{ij}x_j$, we obtained the hole velocity at each time step at every position using the local linear regression.

Figure 3 shows two sample hole trajectories with their velocity diagrams. The holes do not change their traveling directions in Figs. 3(a1) and 3(b1), which is a common feature of all the holes in the defect turbulence. On the other hand, the velocity diagrams are different, with a monotone decline of the hole velocity in Fig. 3(a2), but a local minimum of the hole velocity appearing in Fig. 3(b2). According to the conventional concept of the *coherent structures* [29], the hole velocities are expected to have constant velocities. It is plausible that such behaviors of the hole velocities, as shown in Fig. 3, are caused by energy and/or momentum exchanges of the holes with their surroundings in the birth-death process of the local structures [13].

IV. HOLE VELOCITY FLUCTUATION

Without discriminating each hole, the successive hole velocities in the whole system at each time step are recorded as a time series, as shown in Fig. 4. This hole velocity fluctuation displays the feature of intermittency with large deviations. Indeed, one can recognize two-sided fat tails in the probability distribution. These are denoted as black circles in Fig. 5 and are evaluated with the help of the Rosenblatt-Parzen density estimator to guarantee accuracy of PDF estimation [33].

The hole velocity distribution is fitted by a generalized Cauchy distribution,

$$P_s(v) = \frac{a^{2b-1}}{B(b-1/2,1/2)}\frac{1}{(v^2+a^2)^b}, \qquad (2)$$

where a and b are real parameters, and $B(x,y)$ is the beta function [23], as depicted with the solid line in Fig. 5. The parameters in Eq. (2) are estimated by the maximum likelihood method as $(a,b) = (0.709,2.179)$.

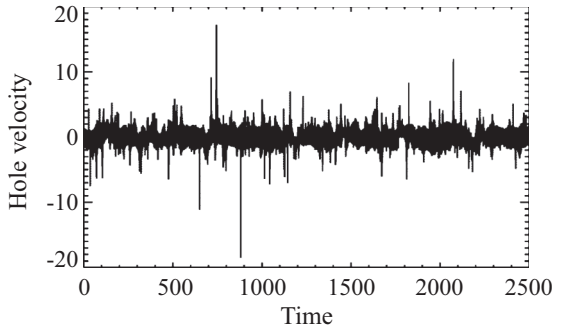

FIG. 4. Hole velocity fluctuation obtained from the successive hole velocities without discriminating each hole in the whole space at each time.

Figure 6 shows the autocorrelation coefficients for the hole velocity fluctuation. It is clear that the autocorrelation coefficients show a nonexponential decay, which implies the existence of long memory. In other words, the conventional GCPs with exponentially decaying ACF cannot give a consistent description on the nature of the hole velocity fluctuation in our simulation.

The mean-square displacement (MSD) is also useful to investigate the characteristics of fluctuating quantity as well as the velocity fluctuation. A relative displacement of the holes is estimated as $X(t) = \int_0^t V(\tau)d\tau$, and then the MSD of $X(t)$ is obtained by the time average on the overall duration T as

$$\langle X^2(t)\rangle_T = \frac{1}{T-t}\int_0^{T-t}[X(\tau+t) - X(\tau)]^2 d\tau. \qquad (3)$$

Figure 7 shows the estimated time-averaged MSD in Eq. (3). In general, the power-law exponent α in $\langle X^2(t)\rangle_T \propto t^\alpha$ classifies diffusive behaviors of fluctuating quantities. In Fig. 7, the exponents α indicate the existences of different scales of the motion in range of superdiffusion ($\alpha > 1$), of which values have been estimated by the least square method (LSM). First the superdiffusive motion appears ($\alpha = 1.53$), then leads to

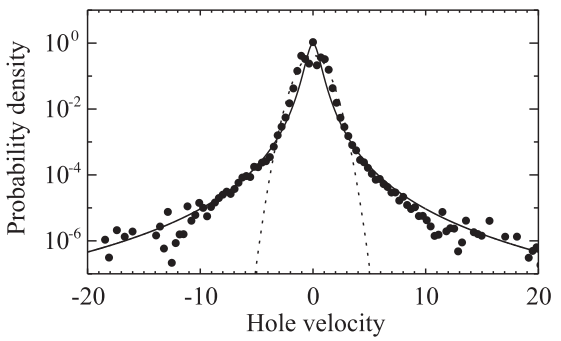

FIG. 5. Probability distribution for the hole velocity fluctuation. The black circles are estimated from the hole velocity fluctuation with the help of the Rosenblatt-Parzen density estimator. The solid line denotes the generalized Cauchy distribution with the parameters $(a,b) = (0.709,2.179)$ estimated by the LSM, of which mean-square error (MSE) is 5.12×10^{-3}. The dashed line denotes the Gaussian distribution with the mean and the variance estimated from the hole velocity fluctuation.

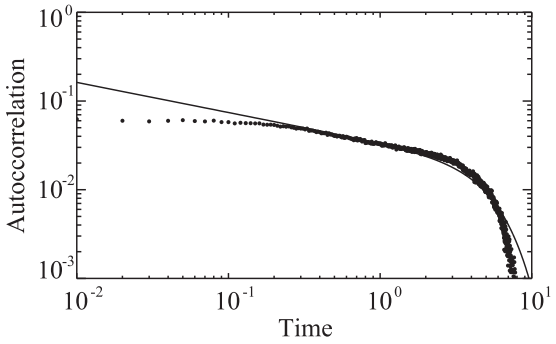

FIG. 6. Autocorrelation coefficients and function for the hole velocity fluctuation. The black circles denote the autocorrelation coefficients for the hole velocity fluctuation estimated from the simulated time series. The solid line denotes the ACF of the NSGCP in Eq. (14) with the estimated parameters $\gamma = 0.429$, $D_a = 0.064$, $D_m = 0.128$, $K = 0.112$, and $\eta = 8.4\times10^4$. The MSE is 4.64×10^{-5}.

nearly ballistic motion ($\alpha = 1.96$) at the midpoint, and eventually displays nearly normal diffusion ($\alpha = 1.05$). A similar picture for random particle systems has been experimentally observed in collective magnetic holes, where superdiffuison with $\alpha = 1.74$ has appeared. Here two other scales can be roughly estimated from Fig. 16 in Ref. [34]—(i) $\alpha = 1.40$ for shorter time scale and (ii) $\alpha = 0.60$ for longer ones.

To describe the above statistical properties, the GCP needs to be generalized with the effect of long memory. There are two candidates for modeling stochastic processes with long memory: stochastic differential equations (SDEs) with subordinator [35] and those with memory functions [15]. Both stochastic processes show non-Markov properties. The former stochastic processes provide long time durations subjected to waiting time distributions between random events, and thus evolution of their PDFs are described by time fractional Fokker-Planck equations. The latter stochastic processes have convolution type or convolutionless type memory functions in SDEs, which are connected by a memory function relation [36]. The corresponding Fokker-Planck equations have time-dependent coefficients.

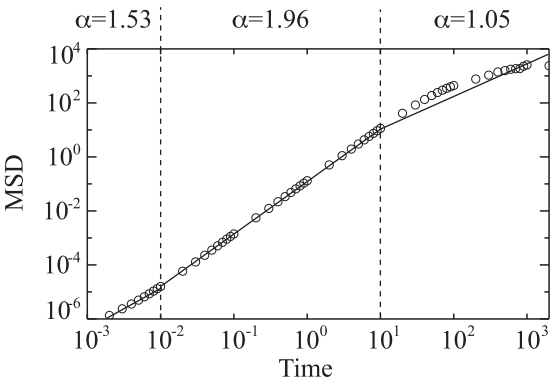

FIG. 7. MSD for the hole velocity fluctuation. White circles denote the MSD obtained by the time averaging in Eq. (3). Solid lines approximate the obtained MSD with power-law exponent as t^α: $\alpha = 1.53$ for $t\in[10^{-3},10^{-2}]$, $\alpha = 1.96$ for $t\in[10^{-2},10^{1}]$, and $\alpha = 1.05$ for $t\in[10^{1},10^{3}]$. The MSE for the time scales are as follows: 1.69×10^{-4} for $t\in[10^{-3},10^{-2}]$, 6.71×10^{-5} for $t\in[10^{-2},10^{1}]$, and 2.00×10^{-2} for $t\in[10^{1},10^{3}]$.

As was shown in Fig. 4, the hole velocity fluctuation has no time durations between random events. Thus it has to be modeled by a SDE with memory functions. As a generalization of the GCPs with non-Markov property, we introduce a nonstationary Îto − type SDE, with convolutionless memory functions, as

$$dV(t) = -(\gamma - D_m)V(t)\nu(t)dt + V(t)\sqrt{2D_m\nu(t)}dW_m(t) + \sqrt{2D_a\nu(t)}dW_a(t), \quad (4)$$

where γ is a real parameter, $W_a(t)$ and $W_m(t)$ are independent standard Brownian motions with their respective intensities $2D_a$ and $2D_m$, and $\nu(t)$ is a time-scaling (memory) function. From here on out, we refer to this stochastic process as a nonstationary generalized Cauchy process (NSGCP). The SDE for the NSGCP in Eq. (4) readily leads to the corresponding nonstationary Fokker-Planck equation as

$$\frac{\partial}{\partial t}P(v,t) = \nu(t)L_{FP}P(v,t), \quad (5)$$

where the operator L_{FP} is defined by

$$L_{FP} = \frac{\partial}{\partial v}(\gamma - D_m)v + \frac{\partial^2}{\partial v^2}(D_m v^2 + D_a). \quad (6)$$

By introducing a rescaled time as

$$\tau = \int_0^t \nu(t')dt', \quad (7)$$

Eq. (5) leads to a conventional Fokker-Planck equation with respect to the rescaled time τ as

$$\frac{\partial}{\partial \tau}P(v,\tau) = L_{FP}P(v,\tau). \quad (8)$$

Thus the solution of Eq. (5) with its statistical quantities can be obtained from Eq. (8). Also, sample paths of Eq. (4) can be obtained from the corresponding conventional Îto − type SDE, by setting $\nu(t) = 1$ in Eq. (4), as $V(t) = V(\tau(t))$. Indeed, the sample path of the NSGCP with respect to the rescaled time τ is expressed by

$$V(\tau) = V(0)e^{-\gamma\tau+\sqrt{2D_m}W_m(\tau)} + \sqrt{2D_a}\int_0^\tau e^{\gamma(\tau'-\tau)-\sqrt{2D_m}[W_m(\tau')-W_m(\tau)]}dW_a(\tau'). \quad (9)$$

The ACF of the NSGCP, which is defined as $C(t) = \langle V(t)V(0)\rangle_{ens}/\langle V(0)V(0)\rangle_{ens}$ with $\langle\cdots\rangle_{ens}$ being the ensemble average, is readily obtained from Eq. (9) as

$$C(t) = \exp[-(\gamma - D_m)\tau(t)]. \quad (10)$$

Thus the specific form of $C(t)$ is determined by $\tau(t)$ in Eq. (7).

The time-scaling function $\nu(t)$ reflects the physical property of time in the system considered. Indeed, as was presented in our previous paper [13], the birth-death process of the local structures including holes has multiple time scales composed of long memory and periodic processes. As a result, one part of the time-scaling function associated with long memory is naturally assumed to have the same form for the case of the birth-death process as

$$\nu_{lm}(t) = \frac{\eta}{1+\eta t}, \quad (11)$$

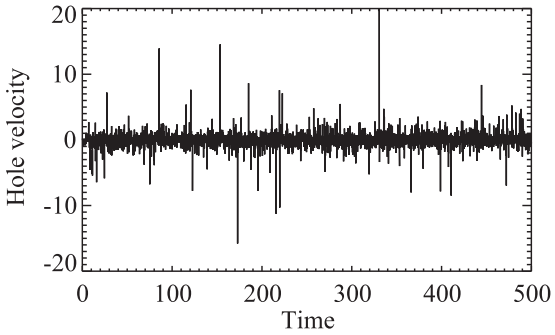

FIG. 8. Sample path of the NSGCP generated from the recurrence formula in Eq. (15) with estimated parameters $\gamma = 0.429$, $D_a = 0.064$, $D_m = 0.128$, $K = 0.112$, and $\eta = 8.4\times10^4$.

with η being a real parameter. In addition, another time scale is expected to exist since each hole displayed particlelike motion with a faster time scale. To express the fast motions, let us introduce

$$v_{bm}(t) = 2Kt, \tag{12}$$

with K being a real parameter, which leads to the rescaled time $\tau = Kt^2$. Employing this rescaled time to the Brownian motion which exhibits the MSD proportional to time after transient motion [37], one can obtain the MSD proportional to the rescaled time, that is, a ballistic motion for a long time. Hence the time-scaling function in Eq. (12) express the particlelike (ballistic) motions of the holes.

Based on the above considerations, the hole velocity fluctuation consists of multitime scale dynamics which can be described by superposition of the time-scaling functions in Eqs. (11) and (12) as

$$v(t) = v_{lm}(t) + v_{bm}(t). \tag{13}$$

The ACF of the NSGCP is given by

$$C(t) = \frac{e^{-(\gamma - D_m)Kt^2}}{(1+\eta t)^{\gamma - D_m}}, \tag{14}$$

and is compared with the autocorrelation coefficients for the hole velocity fluctuation in Fig. 6. The parameters in Eqs. (4) and (14) were estimated using the LSM with $\gamma = 0.429$, $D_a = 0.064$, $D_m = 0.128$, $K = 0.112$, and $\eta = 8.4\times10^4$. It is observed that the ACF in Eq. (14) agrees quite well with the autocorrelation coefficients for the hole velocity fluctuation.

The sample paths of the NSGCP can be numerically simulated from the exact form in Eq. (9). Indeed, the sample paths of the NSGCP in successive discrete times $\{t_n\}_{n\geqslant 0}$ is generated from the recurrence formula

$$V(\tau_{n+1}) = V(\tau_n)e^{-\gamma\Delta\tau + \sqrt{2D_m}\Delta\tau\xi_m} + \sqrt{2D_a\Delta\tau}\,\xi_a e^{\gamma\Delta\tau - \sqrt{2D_m}\Delta\tau\xi_m}, \tag{15}$$

where $\tau_n = v(t_n)$, $\Delta\tau = \tau_{n+1} - \tau_n$, ξ_a, and ξ_m are independent random variables being subjected to the standard Gaussian distribution, as is shown in Fig. 8. It is noted that the feature of intermittency as well as the hole velocity fluctuation shown in Fig. 4 is reproduced satisfactorily.

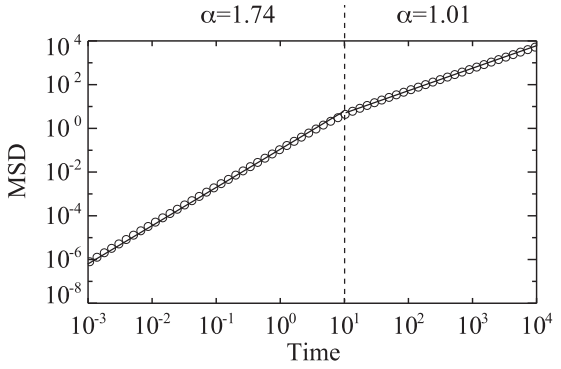

FIG. 9. Theoretical MSD calculated with the representation in Eq. (16). The diffusive behavior changes from superdiffusion with $\alpha = 1.74$ to nearly normal diffusion $\alpha = 1.01$. The MSE are estimated as 9.32×10^{-4} ($t < 10^1$) and 1.81×10^{-4} ($t < 10^1$).

The ensemble-averaged MSD for the successive relative displacements of the holes is given by

$$\langle X^2(t)\rangle_{ens} = \left\langle \int_0^t V(u)du \int_0^t V(u')du' \right\rangle_{ens} = 2\int_0^t (t-s)C(s)ds, \tag{16}$$

with the velocity ACF $C(t)$ in Eq. (14). It can be evaluated by numerical computations as shown in Fig. 9, and is comparable with the time-averaged MSD in Fig. 7 under the assumption of ergodicity. It is observed that the superdiffusive motion with $\alpha = 1.74$ switches to nearly normal diffusion with $\alpha = 1.01$ as with that in Fig. 7. Although the value of α until $t = 10^1$ is different from those in Fig. 7, the value obtained is the same as the average values of α for fast and middle times, namely, $\alpha = 1.53$ and $\alpha = 1.96$. Hence the NSGCP can capture the overall features of the diffusive motions of the holes in the defect turbulence.

V. CONCLUSIONS

The main results of this paper can be summarized as follows. The holes in the defect turbulence displayed particlelike motions with nonconstant velocities, which is caused by energy and/or momentum exchange of the holes with their surroundings in the birth-death process of the local structures. The successive hole velocities without discriminating each hole was recorded as a time series, and was investigated as the hole velocity fluctuation characterized by intermittency, long memory, and superdiffusion. In order to unify all the statistical properties, we proposed the NSGCP with two different time scales of motions. The NSGCP can successfully identify the probability distribution and the autocorrelation coefficients for the hole velocity fluctuation. In addition, it can basically capture the diffusive behavior in the MSD of the holes.

The proposed stochastic model here is expected to describe fluctuations in other nonequilibrium systems. Wave turbulence under annihilation and creation of incoherent structures have been investigated from the equilibrium statistical point of view based on the Boltzmann-Gibbs distribution [38–40]. However, their descriptions with only stationary probability distributions are not enough to characterize dynamical properties of the

wave turbulence. Thus our approach based on SDEs with multiple time-scaling functions like the NSGCP will shed light on both dynamical and statistical properties of spatiotemporal disorders in other nonequilibrium systems.

ACKNOWLEDGMENTS

Y.U. is grateful to Japan Society for the Promotion of Science (JSPS) for Grant-in-Aid for JSPS Fellows (No. 25.374). H.K. is grateful to JSPS for Grant-in-Aid for Challenging Exploratory Research (No. 24650147).

[1] L. E. Reichl, *A Modern Course in Statistical Physics* (University of Texas Press, Austin, 1980).
[2] A. Fiege, B. Vollmayr-Lee, and A. Zippelius, Phys. Rev. E **88**, 022138 (2013).
[3] A. J. Bray, Phys. Rev. E **55**, 5297 (1997).
[4] P. de Anna, T. Le Borgne, M. Dentz, A. M. Tartakovsky, D. Bolster, and P. Davy, Phys. Rev. Lett. **110**, 184502 (2013).
[5] M. C. Cross and P. C. Hohenberg, Rev. Mod. Phys. **65**, 851 (1993).
[6] I. S. Aranson and L. Kramer, Rev. Mod. Phys. **74**, 99 (2002).
[7] M. Cross and H. Greenside, *Pattern Formation and Dynamics in Nonequilibrium Systems* (Cambridge University Press, Cambridge, UK, 2009).
[8] Y. N. Young and H. Riecke, Physica D **176**, 107 (2003).
[9] J. Swift and P. C. Hohenberg, Phys. Rev. A **15**, 319 (1977).
[10] C. Huepe and H. Riecke, Chaos **14**, 864 (2004).
[11] K. E. Daniels, C. Beck, and E. Bodenschatz, Physica D **193**, 208 (2004).
[12] R. Lambiotte and L. Brenig, Phys. Lett. A **345**, 309 (2005).
[13] Y. Uchiyama and H. Konno, Phys. Lett. A **378**, 1350 (2014).
[14] Y. Uchiyama and H. Konno, in *Proceedings of the 45th ISCIE International Symposium on Stochastic Systems Theory and Its Applications, Okinawa, Japan*, edited by S. Sugimoto *et al.* (Institution of Systems, Control and Information Engineers, Kyoto, Japan, 2013).
[15] H. Mori, Prog. Theor. Phys. **33**, 423 (1965).
[16] E. Montroll and G. H. Weiss, J. Math. Phys. **6**, 167 (1965).
[17] J. Klafter and I. M. Sokolov, *First Steps in Random Walks: From Tools to Applications* (Oxford University Press, New York, 2011).
[18] H. Konno, Adv. Math. Phys. **2010**, 504267 (2010).
[19] R. Metzler and J. Klafter, Phys. Rep. **339**, 1 (2000).
[20] C. Tsallis, *Introduction to Nonextensive Statistical Mechanics: Approaching a Complex World* (Springer, New York, 2009).
[21] P. Grassberger, Phys. Rev. Lett. **95**, 140601 (2005).
[22] C. Beck, Philos. Trans. R. Soc. A **369**, 453 (2013).
[23] H. Konno and F. Watanabe, J. Math. Phys. **48**, 103303 (2007).
[24] I. A. Lubashevsky, A. Heuer, R. Friedrich, and R. Usmanov, Eur. Phys. J. B **78**, 207 (2010).
[25] H. Chaté, Nonlinearity **7**, 185 (1994).
[26] H. Chaté and P. Manneville, Physica A **224**, 348 (1996).
[27] J. Yang, *Nonlinear Waves in Integrable and Nonintegrable Systems* (Society for Industrial and Applied Mathematics, Philadelphia, 2010).
[28] N. Bekki and K. Nozaki, Phys. Lett. A **110**, 133 (1985).
[29] M. van Hecke, Phys. Rev. Lett. **80**, 1896 (1998).
[30] Y. Uchiyama and H. Konno, WASET, Int. J. Math. Comput. Phys. Quant. Eng. **7**, 14 (2013).
[31] A. Doelman, Physica D **97**, 398 (1996).
[32] K. E. Daniels and E. Bodenschatz, Chaos **13**, 55 (2003).
[33] A. Janicki and A. Weron, *Simulation and Chaotic Behavior of α-stable Stochastic Processes* (Marcel Dekker, New York, 1994).
[34] S. Clausen, G. Helgesen, and A. T. Skjeltorp, Phys. Rev. E **58**, 4229 (1998).
[35] M. Magdziarz, A. Weron, and K. Weron, Phys. Rev. E **75**, 016708 (2007).
[36] P. Hänggi, H. Thomas, H. Grabert, and P. Talkner, J. Stat. Phys. **18**, 155 (1978).
[37] C. Gardiner, *Stochastic Methods: A Handbook for the Natural and Social Sciences* (Springer, New York, 2009).
[38] H. Sakaguchi, Phys. Rev. E **76**, 017205 (2007).
[39] A. Picozzi and J. Garnier, Phys. Rev. Lett. **107**, 233901 (2011).
[40] J. J. Metzger, R. Fleischmann, and T. Geisel, Phys. Rev. Lett. **112**, 203903 (2014).